Penetration of nonlinear Rossby eddies into South China Sea evidenced by cruise data

Jianyu Hu,[1,2] Quanan Zheng,[2] Zhenyu Sun,[1] and Chang-Kuo Tai[3]

Received 18 August 2011; revised 5 January 2012; accepted 8 January 2012; published 8 March 2012.

[1] From the analyses of the cruise conductivity-temperature-depth profiler and acoustic Doppler current profiler data combined with simultaneous satellite altimeter data and Argo float profiling data, this paper provides evidence for the nonlinear Rossby eddies (NREs) penetrating through the Kuroshio and the Luzon Strait and entering the South China Sea (SCS). A high-salinity water prism in the subsurface layer west of the Luzon Strait was observed in January 2010. The salty prism centered at around 21°N and 118°E has a salinity higher than 34.8 and co-locates with an anticyclonic eddy with a diameter of about 150 km. The water properties of the salty prism are close to those of the Northwest Pacific (NWP) water. The time series of altimeter data and Argo float profiling data indicate that the anticyclonic eddy originates from an NRE that propagates westward from the NWP. The eddy penetrates the Luzon Strait at a speed of about 0.6 m s^{-1} because of the effects of the narrow strait and the Kuroshio-eddy interaction and carries the high-salinity subsurface water from the NWP into the northern SCS.

Citation: Hu, J., Q. Zheng, Z. Sun, and C.-K. Tai (2012), Penetration of nonlinear Rossby eddies into South China Sea evidenced by cruise data, *J. Geophys. Res.*, *117*, C03010, doi:10.1029/2011JC007525.

1. Introduction

[2] The Luzon Strait is located between the Taiwan Island and the Luzon Island as shown in Figure 1. It is an important channel for the water exchange between the South China Sea (SCS) and the northwest Pacific (NWP). From satellite altimeter sea level data, previous investigators have observed that the Rossby waves originating from the NWP within the period of 3–6 months propagate westward to the SCS after passing through the Luzon Strait [*Hu et al.*, 2001]. *Metzger and Hurlburt* [2001], *Li et al.* [2004, 2007], and *Zheng et al.* [2008] further studied the propagation of mesoscale sea level variability or eddy between the NWP and the SCS. *Cai et al.* [2008] discussed the geographical and monthly variability of the phase speed for the first baroclinic Rossby waves in the SCS. Others focused on how the Kuroshio intrudes into the SCS through the Luzon Strait using observation, numerical model, or satellite data [i.e., *Centurioni et al.*, 2004; *Ho et al.*, 2004; *Xue et al.*, 2004; *Yuan et al.*, 2006; *Hu et al.*, 2008]. *Sheu et al.* [2010] examined the conditions when eddies can or cannot freely propagate westward through the Luzon Strait into the SCS using a numerical model. Their results indicate that the eddies are likely to propagate freely through the Luzon Strait during autumn and winter; at that time, the Kuroshio loops westward into the SCS and the potential vorticity across the current is weak. But there are opposite opinions. For example, *He et al.* [2010] thought that no eddy propagates into the SCS via the Luzon Strait from the NWP based on their analysis of 15 years of satellite altimetry data. Recently, *Zheng et al.* [2011] revealed that the mesoscale eddies generated by the nonlinearity of the tropical Rossby waves when approaching the western boundary and defined as nonlinear Rossby eddies (NREs, also as defined by *Chelton et al.* [2011]) do propagate into the SCS. The NREs are able to carry the water mass into the SCS, thus there is a possibility to detect them by cruise observations of water properties.

2. Data and Methods

[3] In January 2010, we carried out a cruise mission for hydrographic observations in the northern SCS onboard R/V *Dong Fang Hong 2*. During the 11 day cruise from 20 to 30 January, we made 28 stations of the conductivity-temperature-depth (CTD) profiler measurements in the sea area west of the Luzon Strait as shown in Figure 1. At each station, the water temperature and salinity (conductivity) were observed with SBE-911 (from Sea-Bird Electronics, Inc.) CTD profiler at a sampling rate of 24 Hz. The specifications of the profiler are as follows: temperature accuracy is 0.001°C, temperature resolution is 0.0002°C, conductivity accuracy is 0.0003 S m^{-1}, resolution 0.00004 S m^{-1}, pressure accuracy 1.0 dbar, and resolution 0.07 dbar. The current was measured underway along the navigation tracks

[1]State Key Laboratory of Marine Environmental Science, College of Ocean and Earth Sciences, Xiamen University, Xiamen, China.
[2]Department of Atmospheric and Oceanic Science, University of Maryland, College Park, Maryland, USA.
[3]National Environmental Satellite, Data, and Information Service, National Oceanic and Atmospheric Administration, Camp Springs, Maryland, USA.

Copyright 2012 by the American Geophysical Union.
0148-0227/12/2011JC007525

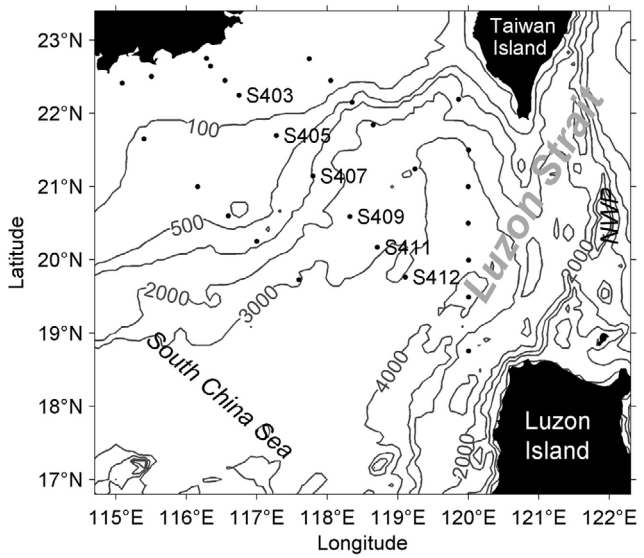

Figure 1. CTD survey stations during a cruise in the northern South China Sea from 20 to 30 January 2010. The survey stations are marked by black dots, and the stations along a main section are coded by S403–S412. The isobaths are in meter.

from one station to another using a shipborne ocean surveyor (OS)-38 (from RD Instruments) acoustic Doppler current profiler (ADCP) at a vertical sampling interval of 16 m. We collected Argo float profiling temperature and salinity data from the Argo data center (http://www.coriolis.eu.org/Data-Services-Products) and the merged altimeter-based daily absolute dynamic topography (MADT) products provided by the Archiving, Validation and Interpretation of Satellite Oceanographic data (Aviso, http://www.aviso.oceanobs.com/en/altimetry/index.html).

[4] Analyzing the cruise observational data in January 2010, we find a high-salinity water prism in the subsurface layer west of the Luzon Strait. Simultaneous satellite altimeter sea level images and Argo float profiling data further reveal that the prism is rotating clockwise. This high-salinity water prism may serve as an evidence for the NRE's penetrating through the Kuroshio and the Luzon Strait and then entering the SCS.

3. Results

3.1. An Anticyclonic Eddy Observed West of the Luzon Strait

[5] Figure 2 shows distributions of temperature and salinity at depths 150, 180, and 200 m, and current vectors at depths 148, 180, and 196 m in the west of the Luzon Strait. From the temperature distribution map, one can see that there is an anticyclonic eddy characterized by a high-temperature core, which is encircled by dense thermals centered at 21.2°N and 117.8°E. The temperature at the eddy core is higher than 23°C, 20°C, and 19°C at three depths 150, 180, and 200 m (Figures 2a–2c). The temperature difference between the eddy core and its outmost edge even exceeds 4°C at 150 and 180 m (Figures 2a and 2b), and 3°C at 200 m (Figure 2c). The temperature gradient reaches 0.09°C km^{-1} at 150 and 180 m southeast of the eddy, implying that there is a strong temperature front there (between stations S411 and S412 in Figure 1).

[6] As shown in Figures 2d–2f, a high-salinity core shows up between 150 and 200 m, corresponding to the warm core. The salty core has a salinity higher than 34.7 and yields a salinity difference of more than 0.15 from its surrounding waters. At 180 m, the salinity at 21.2°N and 117.8°E near station S407 (Figure 1) is even higher than 34.8 (Figure 2e), which is the highest salinity observed at the continental shelf and slope break in the northern SCS during the cruise of January 2010.

[7] The current vectors measured by underway ADCP further confirm that there is an anticyclonic eddy with a diameter of about 150 km (Figure 2g) centered at 21°N and 118.5°E. The tangential speed is about 0.5 m s^{-1} at 148 m and reduces with the depth to about 0.4 m s^{-1} at 180 m and 0.3 m s^{-1} at 196 m (Figures 2h and 2i). The cruise-observed location and size of the anticyclonic eddy coincide with that in the altimeter MADT images shown later in Figure 6.

3.2. A High-Salinity Water Prism Within the Anticyclonic Eddy

[8] Figure 3 shows distributions of temperature, salinity, and potential density measured along two sections on 20–24 January 2010. One section is from station S403 to S412 shown as a red line, and the other is from station S407 to 5901108 shown as a green line in Figure 3d. From Figure 3a, one can see that high-temperature water about 100 m thick occupies the upper layer on the deepwater (southeast) side of the section. The temperature is higher than 24°C at the stations between S407 and S412. A strong thermocline appears at about 100 m at the two end-stations and at about 170 m in the middle section, forming a clear convergence zone at stations S407–S409. Between stations S407 and S409, the thermocline layer is located around 170∼200 m and has an intensity of 0.1°C m^{-1}. On the other hand, Figure 3b shows that in the upper layer (from the surface to 80 m), high-salinity water ($S > 34.5$) appears between S407 and S411, while relatively low-salinity water ($S < 34.0$) appears at station S412, implying an evident salinity front between S411 and S412. The most important phenomenon in the salinity distribution is that a high-salinity water prism exists between 170 and 200 m at stations S407 and S409, with the 34.8 isohaline contour confining the top and the base of the prism. Inside the prism, the salinity is higher than 34.8, which is the highest salinity measured during the cruise. The prism has a thickness of about 30 m at stations S407 and S409 and a diameter of 80 km along the section. It is worth noting that the location of the salty prism is exactly the same as that of the anticyclonic eddy AE shown later in Figure 6d. Such a high-salinity ($S > 34.8$) water prism appearing in the subsurface layer west of the Luzon Strait has rarely been reported.

[9] From Figure 3b, one can see that the abovementioned high-salinity water ($S > 34.8$) is physically connected to the surface water east of the Luzon Strait. The surface water subsides to the subsurface layer when penetrating through the Luzon Strait (as also shown later in Figure 5b), and forms the high-salinity prism at the subsurface layer in the northern SCS. This process is similar to the "Meddy" that is a kind of subsurface mesoscale eddy, which carries warm

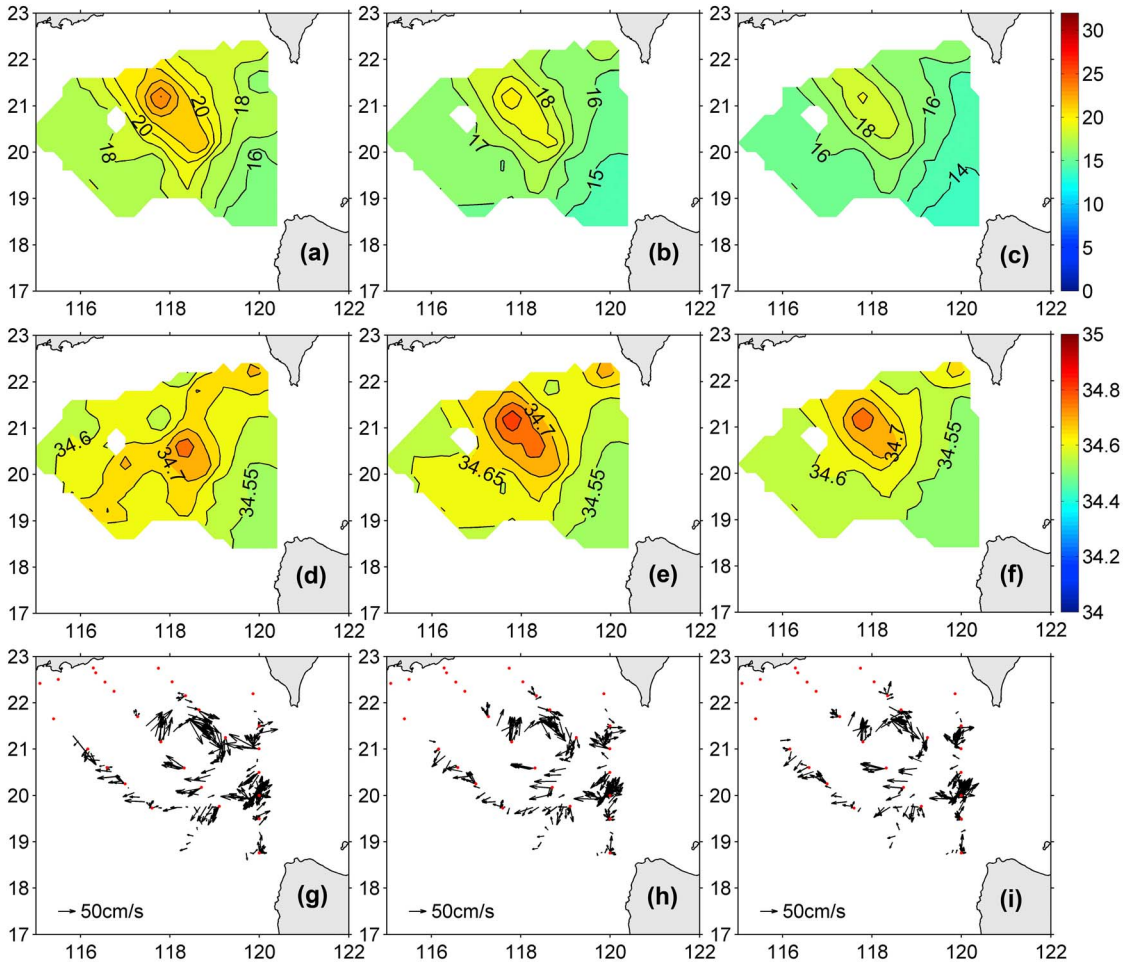

Figure 2. Distributions of temperature (in °C), salinity and current west of the Luzon Strait. Temperature (Figures 2a–2c) and salinity (Figures 2d–2f) at (a, d) 150 , (b, e) 180 , and (c, f) 200 m; ADCP underway measurements along the navigation tracks (g) at 148, (h) 180 , and (i) 196 m, during the cruise from 20 to 30 January 2010. The horizontal axis is in °E longitude and the vertical in °N latitude.

and salty water from the Mediterranean Sea, passes through the Strait of Gibraltar and then subsides in the North Atlantic [*McDowell and Rossby*, 1978; *Richardson et al.*, 2000].

[10] As shown in Figure 3c, low–potential density water exists along section S403–S412, which is vertically homogeneous between the surface layer and 100 m layer. A pycnocline layer has a tendency to slope from 100 m at station S412 down to 150 m at station S407. Below the pycnocline layer, the isopycnals also incline from station S412 to station S407.

[11] Figure 4 shows the temperature profiles, the salinity profiles, and temperature-entropy (T-S) diagrams measured at stations S403–S412. The temperature profiles (Figure 4a) show a vertically homogeneous distribution in the upper layer, and the well-mixed layer reaches depths of 150∼180 m at stations S407 and S409 (red lines in Figure 4a) as a result of the surface water convergence over there (Figure 3a). The salinity profiles at stations S407 and S409 show quite different structures from those at the other stations. At the two stations, the maximum salinity is about 34.8 at depths of around 170∼180 m (red lines in Figure 4b). Below the layer of maximum salinity, the salinity is still greater than that at the other stations. At the layer deeper than 400 m, the salinity becomes almost the same for all deepwater stations.

3.3. Source of the High-Salinity Water

[12] In order to determine the source of the observed high-salinity water, we use the method of T-S diagram analysis. Figure 4c shows T-S diagrams at stations S403–S412, together with three typical T-S diagrams for the SCS water [*Yang et al.*, 1988], the NWP water [*Emery and Dewar*, 1982], and the Kuroshio water in winter [*Yu et al.*, 2000]. For all deepwater stations, the lower portions of the T-S diagrams, which represent the temperature and salinity distributions below 400 m layer, are very close to that of the typical SCS water (in light blue line) and far apart from that of the typical NWP water (in dark blue line) or the typical Kuroshio water in winter (in green line). This implies that the water below 400 m is relatively stable; in other words, the dynamical processes occur mainly above 400 m. On the other hand, the upper portions of the T-S diagrams for stations S407 or S409 (in red lines) are quite different from that of the typical SCS water but close to that of the typical

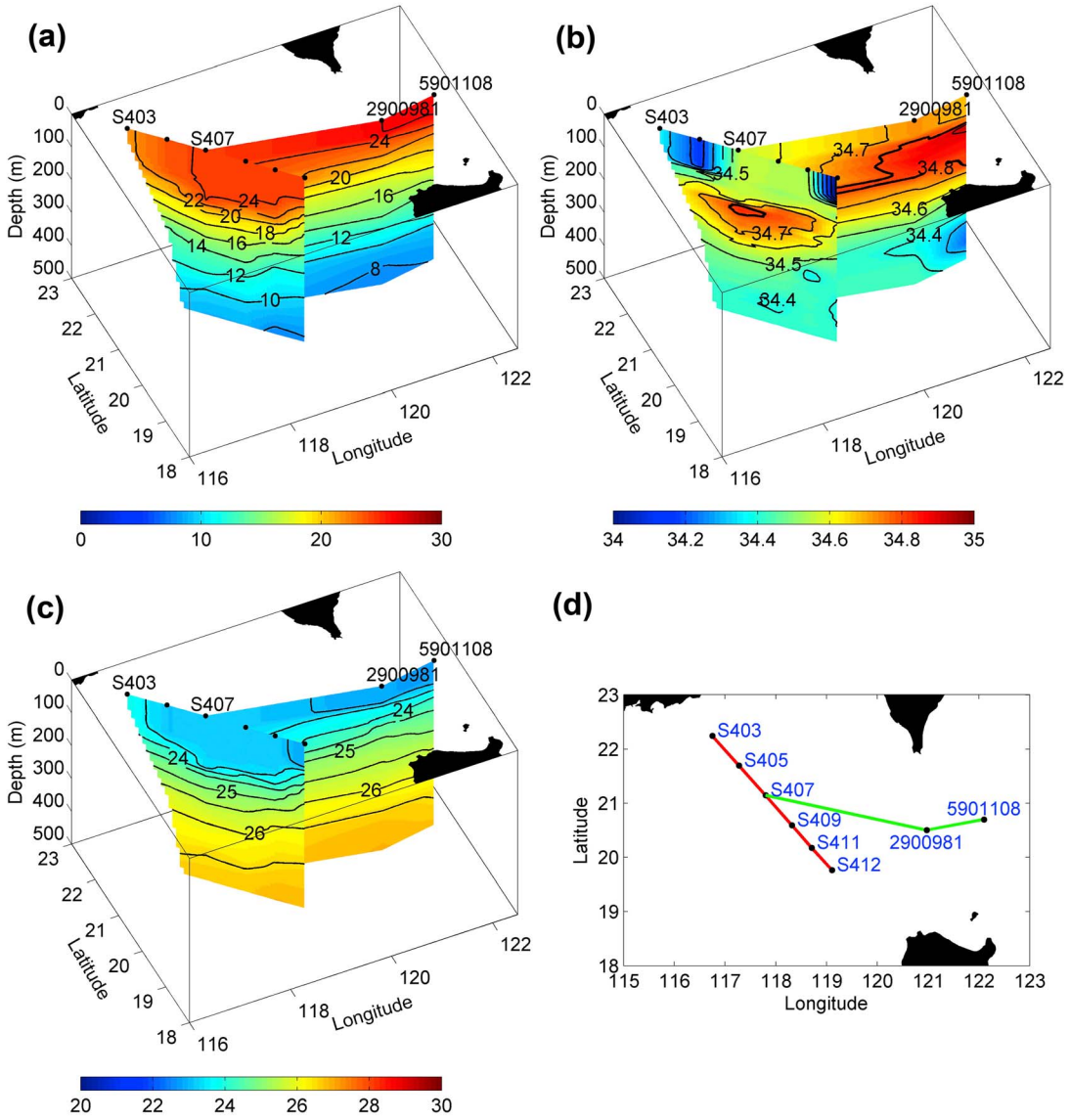

Figure 3. Distributions of (a) temperature, (b) salinity, and (c) potential density (d) at two sections. Section S403–S412 was observed by the CTD profiler during 23–24 January 2010, and section S407-2900981-5901108 by CTD profiler (S407) and Argo floats (2900981 and 5901108) during 20–24 January 2010. Temperature is in °C, and potential density is represented by potential density anomaly (= potential density − 1000) in kg m^{-3}.

NWP water. But the maximum salinity of the salty core at stations S407 and S409 has been 0.10∼0.15 lower than that of the NWP water. We believe that the decrease in the salinity results from the mixing along a long journey of eddy's travel, 500∼600 km from the nearest NWP to the northern SCS with a duration of about 1 month. As for the role of the Kuroshio water in mixing with eddies, in general, it seems reasonable to account for it in the mixing process. However, as observed by *Zheng et al.* [2011] and shown in Figure 6, the true story is that when eddies penetrate through the Luzon Strait, the Kuroshio's normal path is always ruined by interaction with multiple eddies. In the other words, the Kuroshio water has already mixed into eddies. Thus, the NWP water carried by eddies, which is possibly mixed with the Kuroshio water, constitutes a major water source for the NRE propagating into the SCS.

[13] For further tracing the high-salinity water in the subsurface layer of stations S407 and S409, we use a time series of Argo float profiling data whose sampling positions are marked in Figure 5d. The time-depth distributions of temperature, salinity, and potential density near the Luzon Strait are shown in Figures 5a–5c. From Figure 5b, one can see that before 8 January 2010, a salinity front existed between positions 1 and 2 of the central Luzon Strait. The salinity changed from 34.4 to 34.8 within a distance of 30 km. This salinity front appeared from the near-surface layer down to the 200 m layer, which indicates that the high-salinity water originates from a discontinuous source, like an eddy, rather

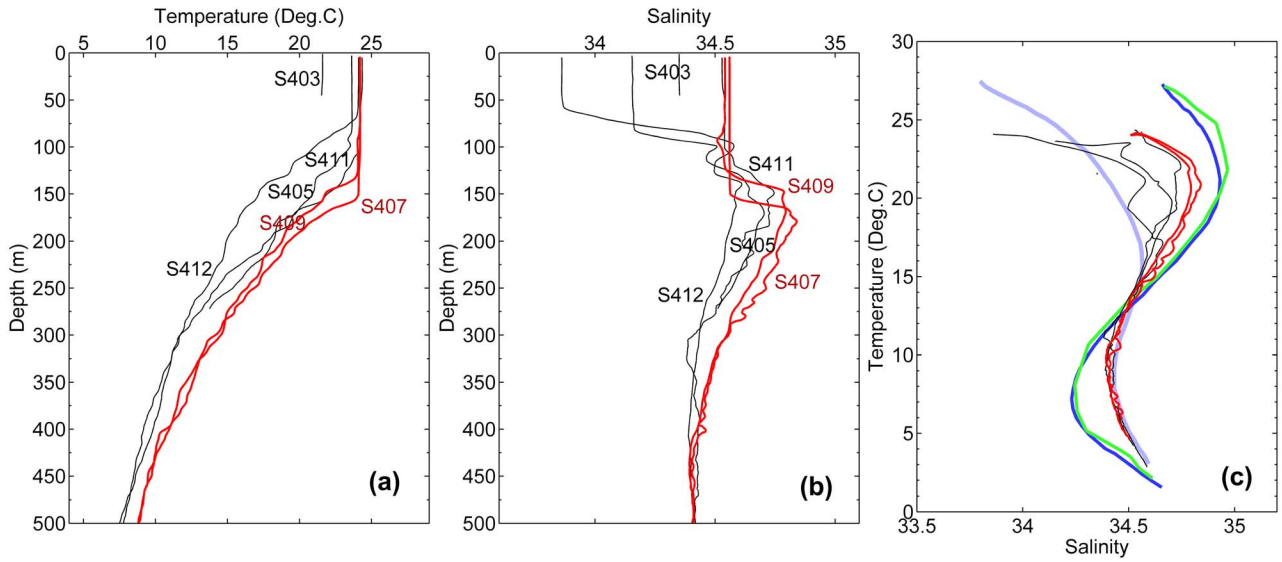

Figure 4. (a) Temperature profiles, (b) salinity profiles, and (c) T-S diagrams at section S403–S412. The temperature and salinity at these stations were observed on 23–24 January 2010. Temperature is in °C. The red lines are for stations S407 and S409. The light blue, dark blue and green lines in Figure 4c are the T-S diagrams for the typical SCS water (redrawn from *Yang et al.* [1988]), the typical NWP water (redrawn from *Emery and Dewar* [1982]), and the typical Kuroshio water in winter (redrawn from *Yu et al.* [2000], respectively.

than a continuous source, like a branch of the Kuroshio. From 8 to 16 January, a high-temperature and low–potential density water subsided from the surface layer to 80 m and formed a convergence zone in the upper layer (Figures 5a and 5c), while a high-salinity water (S > 34.8) appeared at depths between 80 m and 160 m (Figure 5b) in the Luzon Strait. During 24–28 January, the salty water continued to extend along the section within a layer between 100 and 130 m. Remarkably, the high-salinity water (S > 34.8) existed in the subsurface layer around 20.5°N in the central Luzon Strait during 8–28 January.

[14] On the other hand, Figure 3 displays the temperature, salinity, and potential density distributions along another nearly zonal section S407-2900981-5901108 (see green line in Figure 3d), by using CTD cruise data at station S407 and Argo float profiling data of floats 2900981 and 5901108. One can see that a relatively high-salinity water (S > 34.7) extends westward in the subsurface layer and the salinity reaches 34.8 at the depths between 170∼180 m through the whole section from the float 5901108 in the east to the station S407 in the west (Figure 3b). Combining Figures 3b and 5b, one can see that the salty water prism in the subsurface layer of station S407 can be traced back to the east of the Luzon Strait, that is, the NWP.

3.4. Satellite Altimeter Observations

[15] Figure 6 demonstrates the evolution process of an anticyclonic eddy AE west of the Luzon Strait in January 2010. From 14 to 23 January (Figures 6a–6d), AE appeared stationary around 21.5°N and 118.5°E. On 14 January, AE had an MADT value above 250 cm and connected with a large anticyclonic eddy LAE located in the northeast of the Luzon Island. Eddy LAE is an NRE propagating westward from the NWP. As indicated by *Hu et al.* [2001], *Chelton et al.* [2011], and *Zheng et al.* [2011], and shown in Figure 7, the eddy usually propagates westward in the NWP at a phase speed of the Rossby waves. As the ratio of the rotational fluid speed U (about 0.5 m s^{-1}) to the translation speed c (about 0.06 m s^{-1}) is greater than 1 ($U/c > 1$) in the study area, it is reasonable to define the eddy as the nonlinear Rossby eddy. From 17 to 20 January (Figures 6b and 6c), both the area and the maximum MADT value of AE reduced. On 23 January, AE resumed because of the joining of another anticyclonic eddy from the Luzon Strait (AE2 in Figure 6c). It decayed again from 26 January when a large cyclonic eddy LCE moved northward and cut the connection of AE with its parent NRE (LAE in Figure 6). Therefore, the behavior of AE is closely associated with the intermittent contribution of LAE from the northeast of the Luzon Island.

[16] According to Figure 6d, a distinct anticyclonic eddy AE appeared around 21.2°N and 118.2°E on 23 January 2010, when we conducted the CTD observations there. The diameter of this eddy was about 150 km and had a sea level difference of 15 cm between its core and outermost surrounding area. Meanwhile, LAE with its high-MADT tongue extended northwestward like a jet from the NWP to the Luzon Strait. The tongue head of the MADT 230 cm contour line reached 21°N and 120°E in the northern Luzon Strait. Besides, LCE co-existed to the northwest of the Luzon Island, and a cyclonic eddy CE appeared in the sea area southwest of the Taiwan Island. Therefore, four eddies of different scales occur near the Luzon Strait at the same time, implying that the study area is a dynamically active one. Moreover, LAE has remarkably ruined the Kuroshio path as it propagates toward the Luzon Strait. A continuous path of the Kuroshio from the east of the Luzon Island to the east of the Taiwan Island cannot be seen as usual. Under this circumstance, the anticyclonic eddy is likely to propagate freely through the Kuroshio and the Luzon Strait as

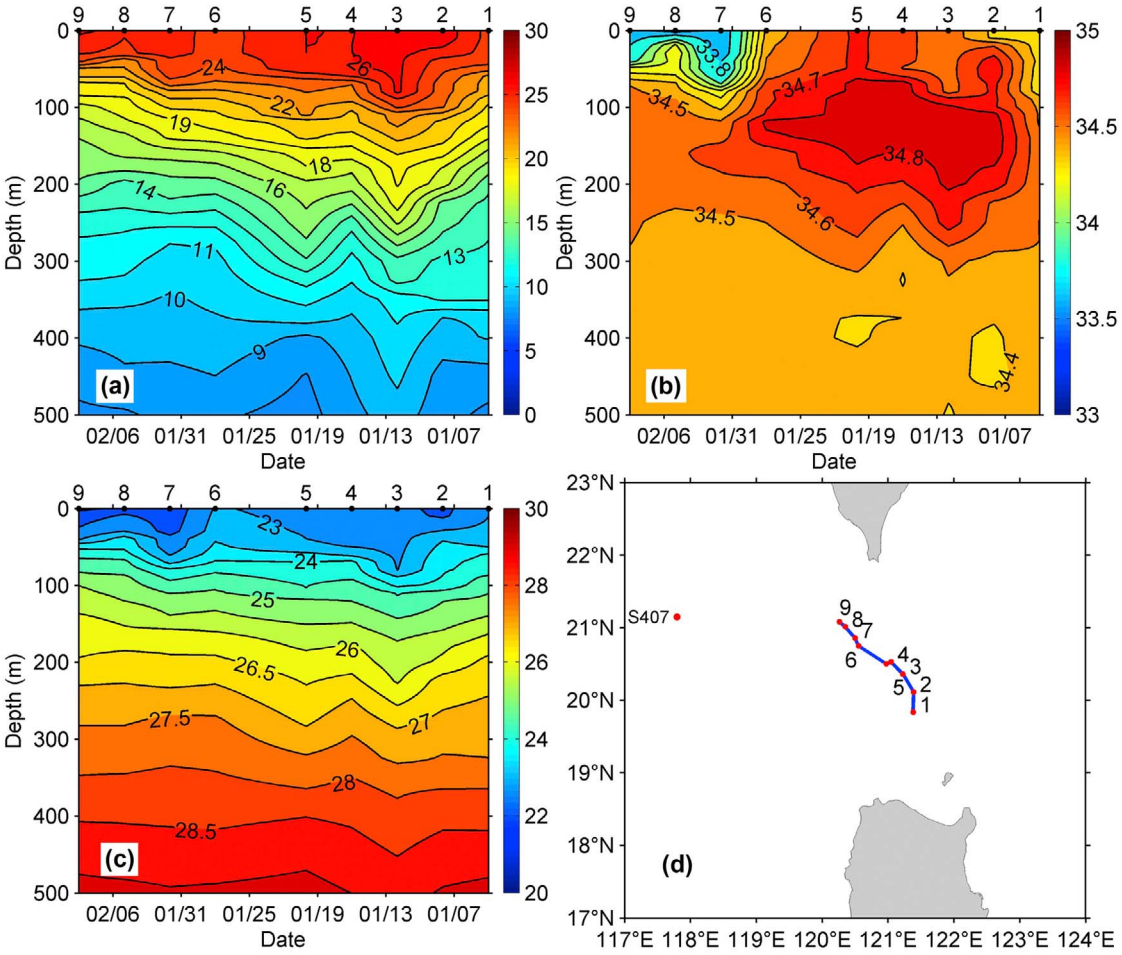

Figure 5. Time-depth distributions of (a) temperature, (b) salinity, and (c) potential density near the Luzon Strait. (d) The dates for Argo float profiling measurement at the specific position from 1 to 9 are on 4, 8, 12, 16, 20, and 28 January and 1, 5, and 9 February 2010, respectively. Temperature is in °C, potential density anomaly (= potential density − 1000) is in kg m^{-3}. The dates (mm/dd) in Figures 5a–5c are set from the right to the left to match the float positions.

described by *Sheu et al.* [2010, Figure 2d]. On 30 January (Figure 6f), the study area west of the Luzon Strait was dominated by LCE. AE and CE were in their decay process.

[17] Figure 7 demonstrates a time-longitude distribution of MADT along a zonal section 21°N from the SCS (117°E) through the Luzon Strait to the NWP (127°E). The sampling time covers a period from 1 December 2009 to 28 February 2010. One can see a remarkable feature before 20 January, which is that three high-MADT belts with nearly parallel crest lines and three low MADT belts were successively distributed from the west to the east. This feature displays a Rossby wave train propagating westward. From Figure 7, we measure the average wavelength as about 300 km and the phase speed as 0.06 m s^{-1}. The Luzon Strait, marked by a black dashed line (Figure 7), plays the role of a dynamical boundary in modulating the Rossby waves. Figure 7 manifests the following facts: (1) The wavelength decreases almost 50% from *O*(400 km) to *O*(200 km) after passing through the strait. (2) The propagation direction of the second wave (Ph2) turns eastward when approaching the strait after 20 January, implying a reflection phenomenon of the Rossby waves on the boundary. (3) The wave (Ph1) in the west of the Luzon Strait has a discontinuous crest line. This suggests that the Rossby waves cannot continuously and freely propagate through the Luzon Strait, which plays the role of a filter. Under this condition, this wave appears in the form of a series of mesoscale eddies in time domain. One of eddies, H4, centered at around 21°N and 118.5°E on 22–25 January is the one we observed during the cruise of January 2010. In other words, the studied eddy is a portion of a Rossby wave, or a constituent of the Rossby wave train. (4) All eddies in the first wave, Ph1, are connected to eddies in Ph2 with high-MADT bridges, such as between H1 and H0, as well as between H4 and H3. This implies a child-parent relationship between them. In other words, eddies in Ph2 are suppliers of mass and momentum for eddies in Ph1.

[18] As shown in Figure 7, eddies in Ph2 usually does not pass through 121°E in the central Luzon Strait. However, during 22–27 December 2009, a high-MADT pattern located at around 120°E (H1 in Figure 7) propagated westward at a phase speed of about 0.06 m s^{-1}, about the same as that of the Rossby waves [*Cai et al.*, 2008]. This high MADT came

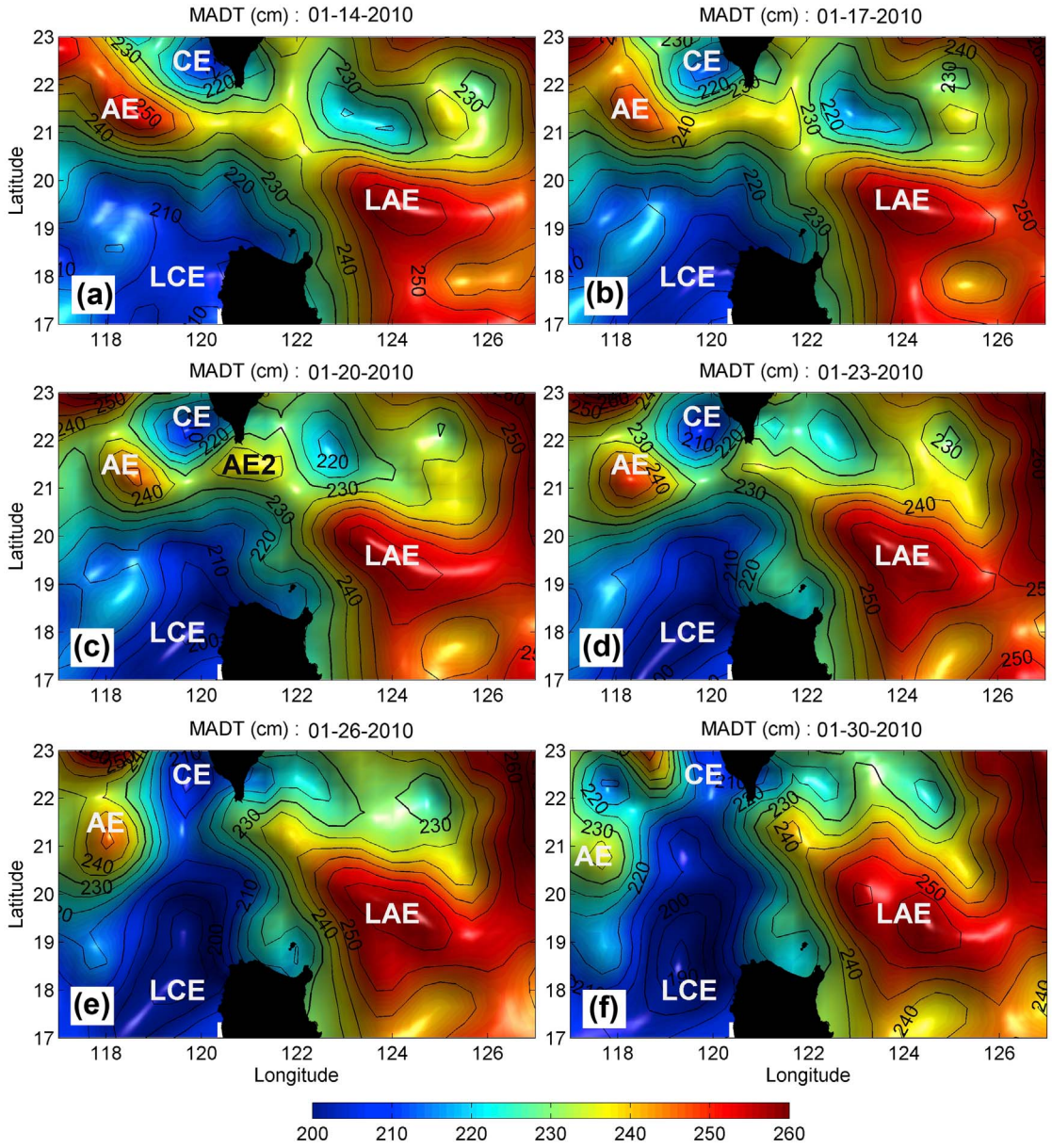

Figure 6. MADT (in cm) maps near the Luzon Strait on (a) 14, (b) 17, (c) 20, (d) 23, (e) 26, and (f) 30 January 2010. AE, CE, LAE and LCE denote anticyclonic eddy, cyclonic eddy, large anticyclonic eddy, and large cyclonic eddy, respectively.

from a high MADT (H0) east of the central Luzon Strait, which penetrated the Luzon Strait at a phase speed of about 0.6 m s^{-1} (shown as a black arrow) as affected by the narrow strait and the Kuroshio-eddy interaction proposed by *Zheng et al.* [2011].

[19] During 12–18 January 2010, there was a high MADT around 119°E (H2) west of the Luzon Strait from 12 January, then it propagated westward (shown as a black arrow) at a phase speed of about 0.06 m s^{-1}, which was about the same as that of the Rossby waves in the northern SCS [*Hu et al.*, 2001; *Cai et al.*, 2008]. From 13 January, a high MADT (H3) intruded westward quickly through the Luzon Strait at a phase speed of 0.65 m s^{-1} (shown as a red arrow), combined with H2, and formed a new eddy H4 centered at around 21°N and 118.5°E on 22–25 January. From late January, a low MADT pattern existed in the Luzon Strait, lasted for more than 1 month, and separated the high-MADT areas on the west and east of the Luzon Strait.

[20] Evidently, the NRE penetrates through the central Luzon Strait as propagating westward brings the NWP water from the surface layer to the subsurface layer and propagates further westward to 21°N and 118.5°E.

4. Discussion

[21] In recent years, there have been many studies focusing on warm or anticyclonic eddies in the northeastern SCS and around the Luzon Strait [*Jia and Liu*, 2004; *Jia et al.*, 2005]. However, the generation mechanisms and the water sources of eddies still remain debatable. There are three

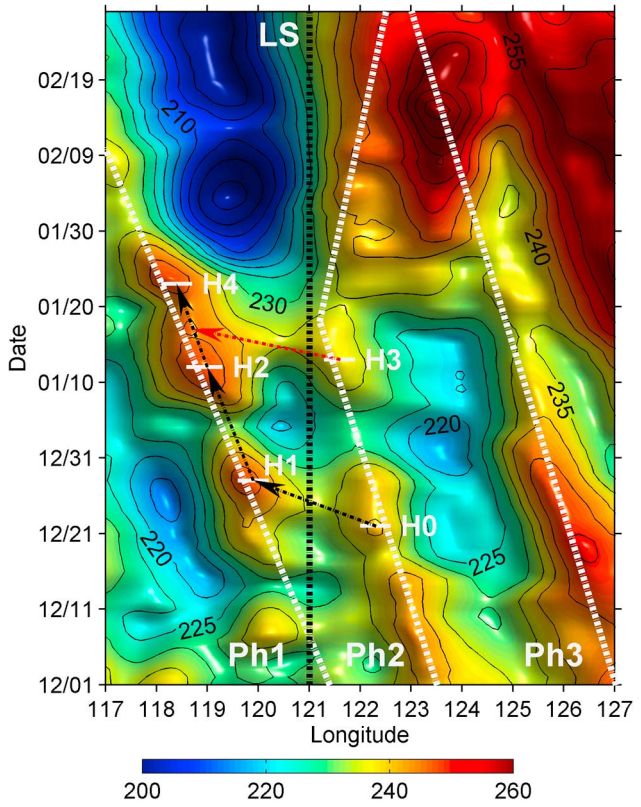

Figure 7. Time-longitude distribution of MADT (in cm) along 21°N from 117°E (the northern SCS) to 127°E (NWP) The sampling time covers the period from 1 December 2009 to 28 February 2010. The black dashed line represents the location of the central line of the Luzon Strait (LS). The white dashed lines (Ph1, Ph2, and Ph3) represent the isophase lines of the Rossby waves.

major viewpoints: (1) eddies are detached or shed rings from the Kuroshio, (2) eddies are locally generated in the northeastern SCS, and (3) eddies are generated by the nonlinearity of the Rossby waves from the NWP and propagate westward into the SCS through the Luzon Strait.

[22] *Li et al.* [1998] reported an anticyclonic ring with a scale of about 150 km and a warm core centered at about 21°N and 117.5°E just off the continental slope in the northeastern SCS in September 1994. They suggested that the ring was of Kuroshio origin. We believe that there is a similarity between this eddy and the case of this study, but we hypothesize a different origin, the NWP.

[23] *Yuan et al.* [2007] identified a Luzon warm eddy and suggested that the eddy was generated off the northwestern coast of the Luzon Island in summer and was facilitated by the southerly wind and minimum wind curl. They argued that the anticyclonic eddy observed by *Li et al.* [1998] was the Luzon warm eddy generated from the northwest of the Luzon Island instead of being detached from the Kuroshio. *Chen et al.* [2010] recently analyzed the seasonal variation of the Luzon warm eddy, showing that the eddy extended vertically down to the depth of 500 m, with a high-temperature anomaly of 5°C and a low-salinity anomaly of 0.5 near the thermocline, and a maximum tangential speed of 0.6 m s^{-1} at its uppermost 200 m. This Luzon warm eddy generally forms in July, intensifies in August and September, propagates westward approximately along 19°N from northwest of the Luzon Island to southeast of the Hainan Island at a mean speed of 6.6 cm s^{-1} in October, and then disappears in February. The typical feature of the Luzon warm eddy is a relatively low salinity at the subsurface layer. Clearly, that eddy is completely distinct from the case of this study, which is characterized by a high-salinity core.

[24] *Wang et al.* [2008] described two anticyclonic eddies in the northeastern SCS in winter 2003–2004. One was located at the same location as the eddy AE of the present study. But they suggested that the eddy was generated in the interior SCS. Another eddy near the Luzon Strait they believed was shed from a Kuroshio meander. *Zhuang et al.* [2010] proposed that mesoscale eddies propagate southwestward in the west of the Luzon Strait. Although eddies are most active in winter, their southwestward migration steered by the bathymetry occurs throughout the year.

[25] The anticyclonic eddy reported in this paper is completely different from the aforementioned case analyses. The eddy has a salinity as high as 34.8 in the subsurface layer, which is the highest salinity ever observed in the northern SCS. As the large anticyclonic eddy (such as LAE in Figure 6) propagates westward, it ruins the normal northward path of the Kuroshio. Then a portion of LAE is pushed westward like a pulse through the Luzon Strait at a phase speed of about 0.6 m s^{-1}. Therefore, the anticyclonic eddy in the northern SCS originates from a westward propagating NRE, rather than sheds from the Kuroshio that is actually temporarily disappearing, forced by the large anticyclonic eddy LAE [*Zheng et al.*, 2011]. The eddy continues propagating westward at a phase speed the same as that of the Rossby waves and reaches the northern SCS. Our cruise observation just captured this anticyclonic eddy in the subsurface layer at 21°N and 118.5°E as a salty prism with salinity higher than 34.8. The temperature and salinity structures show that the observed NRE reaches as deep as 400 m, and the evident high-salinity water core appears at the depths of 180∼200 m. The present study, however, is limited to the diagnostic analysis based on the interpretations of observations. The purpose of this paper is only to reveal new evidences for clarifying the physical properties and origins of eddies in the SCS, which are distinct from the previous concepts and understandings. Dynamical and quantitative analyses are necessary for drawing the final conclusions, thus they will be our future efforts.

5. Summary

[26] Using cruise CTD and ADCP data observed in January 2010, combined with the satellite altimeter data and Argo float profiling data, this paper analyzes the mesoscale eddy dynamics in the northern SCS. The cruise data analysis results reveal a high-salinity water prism centered at 21°N and 118.5°E in the subsurface layer west of the Luzon Strait. The salty prism is characterized by the following: (1) the salinity is higher than 34.8, (2) it is located at the center of an anticyclonic eddy with a diameter of about 150 km, and (3) the water properties of the eddy are close to those of the NWP water. The satellite altimeter time series data analysis indicates that the anticyclonic eddy is

originating from a large NRE that propagates westward from the NWP. A portion of the large eddy intermittently penetrates the Luzon Strait and forms a new eddy in the northern SCS. Thus, the new eddy is still characterized by a high-salinity water core, though suffering strong mixing with surrounding waters along a travel of 500–600 km from the NWP to the northern SCS.

[27] The findings of this study represent a new step for understanding the interaction between the NRE and the Kuroshio and the penetration of the eddy through the Kuroshio and the Luzon Strait into the SCS. Eddies would have significant impacts on the SCS circulation because they carry the water mass and the heat from the NWP to the SCS. Thus, it is worth further clarifying the occurrence conditions and annual occurrence rate of the NRE penetration through the Luzon Strait. In order to do so, long-time mooring observation and fine-resolution modeling are proposed for future research.

[28] **Acknowledgments.** This study is supported by the National Basic Research Program of China through projects of 2009CB421208 and 2007CB411803 and the Natural Science Foundation of China through projects of 40976013 and 41121091 (for J. Hu), by the United States of America National Oceanic and Atmospheric Administration National Environmental Satellite, Data, and Information Service Ocean Remote Sensing Funding Program 3000-11-03241 (for Q. Zheng and C.-K. Tai). We thank the crew of R/V *Dong Fang Hong 2* and all the cruise participants for help with the field work and X. G. Guo for providing ADCP data of Figures 2g–2i. We also appreciate the Argo data center and the Aviso center for their online data. We are grateful to the two anonymous reviewers for their valuable suggestions and comments for improving the manuscript.

References

Cai, S. Q., X. M. Long, R. H. Wu, and S. G. Wang (2008), Geographical and monthly variability of the first baroclinic Rossby radius of deformation in the South China Sea, *J. Mar. Syst.*, *74*, 711–720, doi:10.1016/j.jmarsys.2007.12.008.

Centurioni, L. R., P. P. Niiler, and D. K. Lee (2004), Observation of inflow of Philippine Sea surface water into the South China Sea through the Luzon Strait, *J. Phys. Oceanogr.*, *34*, 113–121, doi:10.1175/1520-0485(2004)034<0113:OOIOPS>2.0.CO;2.

Chelton, D. B., P. Gaube, M. G. Schlax, J. J. Early, and R. M. Samelson (2011), The influence of nonlinear mesoscale eddies on near-surface oceanic chlorophyll, *Science*, *334*, 328–332, doi:10.1126/science.1208897.

Chen, G. X., Y. J. Hou, X. Q. Chu, and P. Qi (2010), Vertical structure and evolution of the Luzon warm eddy, *Chin. J. Oceanol. Limnol.*, *28*, 955–961, doi:10.1007/s00343-010-9040-3.

Emery, W. J., and J. S. Dewar (1982), Mean temperature-salinity, salinity-depth and temperature-depth curves for the North Atlantic and the North Pacific, *Prog. Oceanogr.*, *11*, 219–305, doi:10.1016/0079-6611(82)90015-5.

He, Y. H., S. Q. Cai, and S. G. Wang (2010), The correlation of the surface circulation between the western Pacific and the South China Sea from satellite altimetry data, *Int. J. Remote Sens.*, *31*, 4757–4778, doi:10.1080/01431161.2010.485137.

Ho, C.-R., Q. Zheng, N.-J. Kuo, C.-H. Tsai, and N. E. Huang (2004), Observation of the Kuroshio intrusion region in the South China Sea from AVHRR data, *Int. J. Remote Sens.*, *25*, 4583–4591, doi:10.1080/0143116042000192376.

Hu, J. Y., H. Kawamura, H. S. Hong, F. Kobashi, and D. X. Wang (2001), 3∼6 months variation of sea surface height in the South China Sea and its adjacent ocean, *J. Oceanogr.*, *57*, 69–78, doi:10.1023/A:1011126804461.

Hu, X., X. Xiong, F. Qiao, B. Guo, and X. Lin (2008), Surface current field and seasonal variability in the Kuroshio and adjacent regions derived from satellite-tracked drifter data, *Acta Oceanol. Sin.*, *27*, 11–29.

Jia, Y., and Q. Y. Liu (2004), Eddy shedding from the Kuroshio bend at Luzon Strait, *J. Oceanogr.*, *60*, 1063–1069, doi:10.1007/s10872-005-0014-6.

Jia, Y., Q. Y. Liu, and W. T. Liu (2005), Primary study of the mechanism of eddy shedding from the Kuroshio bend in Luzon Strait, *J. Oceanogr.*, *61*, 1017–1027, doi:10.1007/s10872-006-0018-x.

Li, L., W. D. Nowlin Jr., and J. L. Su (1998), Anticyclonic rings from the Kuroshio in the South China Sea, *Deep Sea Res., Part I*, *45*, 1469–1482, doi:10.1016/S0967-0637(98)00026-0.

Li, L., C. Jing, and D. Zhu (2007), Coupling and propagating of mesoscale sea level variability between the western Pacific and the South China Sea, *Chin. Sci. Bull.*, *52*, 1699–1707, doi:10.1007/s11434-007-0203-3.

Li, Y. C., L. Li, C. S. Jing, and W. L. Cai (2004), Temporal and spatial variabilities of sea surface heights in the northeastern South China Sea, *Chin. Sci. Bull.*, *49*, 491–498.

McDowell, S. E., and H. T. Rossby (1978), Mediterranean water: An intense mesoscale eddy off the Bahamas, *Science*, *202*, 1085–1087, doi:10.1126/science.202.4372.1085.

Metzger, E. J., and H. E. Hurlburt (2001), The nondeterministic nature of Kuroshio penetration and eddy shedding in the South China Sea, *J. Phys. Oceanogr.*, *31*, 1712–1732, doi:10.1175/1520-0485(2001)031<1712:TNNOKP>2.0.CO;2.

Richardson, P. L., A. S. Bower, and W. Zenk (2000), A census of Meddies tracked by floats, *Prog. Oceanogr.*, *45*, 209–250, doi:10.1016/S0079-6611(99)00053-1.

Sheu, W.-J., C.-R. Wu, and L.-Y. Oey (2010), Blocking and westward passage of eddies in the Luzon Strait, *Deep Sea Res., Part II*, *57*, 1783–1791, doi:10.1016/j.dsr2.2010.04.004.

Wang, D. X., H. Z. Xu, J. Lin, and J. Y. Hu (2008), Anticyclonic eddies in the northeastern South China Sea during winter 2003/2004, *J. Oceanogr.*, *64*, 925–935, doi:10.1007/s10872-008-0076-3.

Xue, H. J., F. Chai, N. Pettigrew, D. Y. Xu, M. Shi, and J. P. Xu (2004), Kuroshio intrusion and the circulation in the South China Sea, *J. Geophys. Res.*, *109*, C02017, doi:10.1029/2002JC001724.

Yang, Y. H., L. Li, and Z. D. Wang (1988), Characteristics of average T-S, S-Z and T-Z in the South China Sea, *Trop. Oceanol.*, *7*, 54–59.

Yu, H. H., Y. C. Yuan, J. L. Su, Y. T. Miao, and L. L. Shen (2000), Hydrographic characteristics of the Kuroshio east of Taiwan Island and its adjacent regions during the winter of 1997, *Oceanogr. China*, *12*, 30–36.

Yuan, D., W. Han, and D. Hu (2006), Surface Kuroshio path in the Luzon Strait area derived from satellite remote sensing data, *J. Geophys. Res.*, *111*, C11007, doi:10.1029/2005JC003412.

Yuan, D. L., W. Q. Han, and D. X. Hu (2007), Anticyclonic eddies northwest of Luzon in summer–fall observed by satellite altimeters, *Geophys. Res. Lett.*, *34*, L13610, doi:10.1029/2007GL029401.

Zheng, Q., H. Lin, J. Meng, X. Hu, Y. T. Song, Y. Zhang, and C. Li (2008), Sub-mesoscale ocean vortex trains in the Luzon Strait, *J. Geophys. Res.*, *113*, C04032, doi:10.1029/2007JC004362.

Zheng, Q. A., C. K. Tai, J. Y. Hu, H. Y. Lin, R.-H. Zhang, F.-C. Su, and X. F. Yang (2011), Satellite altimeter observations of nonlinear Rossby eddy–Kuroshio interaction at the Luzon Strait, *J. Oceanogr.*, *67*, 365–376, doi:10.1007/s10872-011-0035-2.

Zhuang, W., Y. Du, D. X. Wang, Q. Xie, and S. P. Xie (2010), Pathways of mesoscale variability in the South China Sea, *Chin. J. Oceanol. Limnol.*, *28*, 1055–1067, doi:10.1007/s00343-010-0035-x.

J. Hu and Z. Sun, State Key Laboratory of Marine Environmental Science, College of Ocean and Earth Sciences, Xiamen University, Xiamen, Fujian 361005, China. (hujy@xmu.edu.cn)

C.-K. Tai, National Environmental Satellite, Data, and Information Service, National Oceanic and Atmospheric Administration, 5200 Auth Rd., Camp Springs, MD 20746, USA.

Q. Zheng, Department of Atmospheric and Oceanic Science, University of Maryland, College Park, MD 20742, USA.